

Universality of entanglement in gluon dynamics

Claudia Núñez^{1*}, Alba Cervera-Lierta² and José Ignacio Latorre³

¹ Institut Cartogràfic i Geològic de Catalunya, Barcelona, Spain

² Barcelona Supercomputing Center, Barcelona, Spain

³ Centre for Quantum Technologies, National University of Singapore, Singapore

* claudia.nunezgarrido@outlook.es

Abstract

Entanglement of fundamental degrees of freedom in particle physics is generated *ab initio* in scattering processes. We find that in the case of a pure $SU(N)$ gauge theory, two gluons in a product state can become maximally entangled in their polarizations as the result of three- and four-gluon vertex interactions. Remarkably, the amount of entanglement among gluon polarizations is independent of the color degree of freedom. We also find that a small deviation of the relative weight between three- and four-gluon vertices would prevent the generation of maximal entanglement. This can be seen as a small piece of a possible *it from qubit* principle underlying fundamental interactions.

Copyright attribution to authors.

This work is a submission to SciPost Physics.

License information to appear upon publication.

Publication information to appear upon publication.

Received Date

Accepted Date

Published Date

¹

Contents

³ 1	Introduction	2
⁴ 2	A figure of merit for entanglement	3
⁵ 3	Tree-level gluon scattering amplitudes	4
⁶ 4	Generation of entanglement	6
⁷ 5	Exploring a MaxEnt principle	6
⁸ 6	Conclusions	8
⁹ 7	Acknowledgements	9
¹⁰ A	Conventions	10
¹¹ A.1	Kinematics	10
¹² A.2	Feynman rules	11
¹³ B	Polarized amplitudes $gg \rightarrow gg$	11
¹⁴ B.1	s-channel	11
¹⁵ B.2	t-channel	12
¹⁶ B.3	u-channel	12

17	B.4 4-point	13
18	C Total amplitudes with vertex modification	13
19	References	13
20		
21		

22 1 Introduction

23 Entanglement is a technical word reserved to describe correlations in quantum mechanics,
24 specifically those emerging for a quantum state made of two or more subsystems that cannot
25 be described as a classical combination of the states of each subpart. Entanglement is a core
26 feature in quantum physics that, by means of violation of Bell inequalities [1], discriminates
27 between classical and quantum physics.

28 A question arises on the origin of entanglement in the basic processes of Nature. Can the
29 fundamental interactions in the Standard Model create entangled states? If so, do they pro-
30 vide mechanisms to obtain maximal entanglement from non-entangled states? The ultimate
31 question would correspond to understand whether entanglement may turn to be a candidate
32 to formulate a novel principle in physics, one demanding that physics is quantum, not classical.

33 This is the thread of thought explored in Refs. [2, 3] and the present work. The authors
34 focused in QED and weak interactions, studying the correlations between helicity states in
35 two-body scattering processes and decays. For QED interactions, it was found that maximal
36 entangled states are created from a product state by two mechanisms: *s*-channel processes at
37 high energies where the virtual photon carries equal overlaps of the helicities of the final state
38 particles; and the indistinguishable superposition of *t* and *u*-channels, valid for all energies.
39 The latter mechanism justifies why the low-energy interaction between two spins, namely
40 the Heisenberg model, is able to generate maximal entanglement. It was also shown that
41 requiring the generation of maximal entangled states leads to reproducing the exact QED
42 photon-electron vertex. Such a result suggests the idea of exploring some kind of Maximal
43 Entanglement Principle (MaxEnt) as a guiding element to construct quantum theories. Finally,
44 it was observed that maximal entanglement favors a weak mixing angle of $\frac{\pi}{6}$, very close to the
45 Standard Model value. A similar result is obtained in Ref. [4], where maximal entanglement
46 also favors a weak mixing angle of $\frac{\pi}{6}$ for the three-body Higgs boson decay $H \rightarrow \gamma l \bar{l}$ at 1-loop
47 level. The generation of entanglement in QED scattering processes has also been studied in
48 Refs. [5–7] where the authors do not restrict to initial product states.

49 Further work has also been done in studying entanglement in positronium [8], charmon-
50 ium [9, 10] and Higgs boson [11–14] decays, generation of kaon [15], B meson [16], τ
51 lepton [17] and top quark [18–20] pairs, as well as in neutrino oscillations [21, 22] and vec-
52 tor boson scattering [23], to propose Bell tests that could be experimentally verified. For top
53 quarks, there have also been studies in quantum tomography techniques [24] and, recently,
54 entanglement between a top quark pair has been experimentally detected by the ATLAS and
55 CMS collaborations at the LHC [25–27]. The production of these top quarks comes primar-
56 ily from gluon interactions in these collisions. Then, since top quarks decay faster than their
57 hadronization, they transfer their spin properties to their decay products, which allows the es-
58 timation of their entanglement properties from the measurement of the angular dependence
59 of the detected jets. Therefore, the phenomenology surrounding gluon scattering is of spe-
60 cial interest for high-energy physics experimentalists. Violations of Bell inequalities have also
61 been obtained experimentally in charmonium [28] and B meson [29, 30] decays. The use of

62 entanglement in particle interactions has also been proposed to constrain new physics beyond
 63 the Standard Model using LHC measurements [31–37].

64 We should also note a line of research complementary to the study of a possible MaxEnt
 65 principle, where the interplay between entanglement suppression in scattering processes and
 66 the emergence of global symmetries has been explored in Standard Model [38–40] and beyond
 67 the Standard Model [41, 42] interactions, as well as its relation with symmetry-breaking effects
 68 as quark and lepton mixing [43], and MaxEnt [42].

69 In this work, we take a step further focusing on pure Yang-Mills gluon dynamics. We
 70 compute the polarized amplitudes for gluon scattering at tree-level using the three- and four-
 71 gluon couplings. Then, using the concurrence as a figure of merit, we show that entanglement
 72 is only generated when the initial product state presents opposite polarizations. Maximal
 73 entangled states are only produced in the case where the scattering angle is $\theta = \frac{\pi}{2}$. Then, the
 74 final states are always maximally entangled, independently of the color of the gluons involved
 75 in the process. This result points at some structure in pure Yang-Mills theory that imposes a
 76 sort of universal creation of entanglement, independent of the particular gauge group at play.

77 It is tantalizing to investigate whether the relation between the three- and four-gluon ver-
 78 tices, as dictated by gauge symmetry, can be imposed from a MaxEnt Principle. While this
 79 is not the case in full generality, we demonstrate that a clear and robust relationship does
 80 emerge. This result suggests a deep relation between local symmetries and entanglement.

81 It must be made clear that gluons are not asymptotically free particles. It is thus not pos-
 82 sible to perform a Bell test based on the gluon polarizations, as it is done for photons. The
 83 idea, though, is that maximal entanglement is indeed generated and conditions the subse-
 84 quent evolution of the full system. In this sense, we here analyze the conditions for maximal
 85 entanglement to be generated.

86 The structure of this paper goes as follows. In Sect. 2, we introduce a figure of merit to
 87 quantify entanglement for two particle scattering processes. In Sect. 3 we present the results
 88 obtained for the total polarized scattering amplitudes in the gluon scattering. Sect. 4 is cen-
 89 tered on the analysis of the generation of entanglement in these processes. Sect. 5 is devoted to
 90 verify the way the relative weight between three- and four-gluon vertices affect entanglement,
 91 and shows how a MaxEnt principle works in this scenario. Our conclusions are presented in
 92 Sect. 6. Some additional information and conventions are included in App. A. App. B collects
 93 the complete set of polarized amplitudes computed for each channel. App. C lists the complete
 94 set of polarized amplitudes when the balance between the 3- and 4-gluon vertices is modified.
 95 We should note that Ref. [3] also presents an analysis of the gluon scattering process. The
 96 present work presents new results and conclusions.

97 2 A figure of merit for entanglement

98 In order to quantify entanglement in gluon scattering it is necessary to specify the quantum
 99 degrees of freedom at stake as well as to provide a precise figure of merit. We shall discuss
 100 entanglement in terms of polarizations of gluons, and entanglement will be quantified using
 101 the concurrence obtained from the coefficients of the superposition of final states.

102 Considering that the polarization of the gluons can take two values, right-handed (R) and
 103 left-handed (L), we can describe the incoming and outgoing states as two qubit states with
 104 basis $\{|R\rangle, |L\rangle\}$. After the interaction, the final state will be a superposition of all possible
 105 combinations of the two polarizations. Therefore, for an initial product state $|RR\rangle, |RL\rangle, |LR\rangle$
 106 or $|LL\rangle$, the final state $|\psi_f\rangle$ can be written as

$$|\psi_f\rangle \sim \mathcal{M}_{\psi_i \rightarrow RR}|RR\rangle + \mathcal{M}_{\psi_i \rightarrow RL}|RL\rangle + \mathcal{M}_{\psi_i \rightarrow LR}|LR\rangle + \mathcal{M}_{\psi_i \rightarrow LL}|LL\rangle, \quad (1)$$

107 where $\mathcal{M}_{\psi_i \rightarrow AB}$ is the scattering amplitude at tree level for the process where the final state

108 is $|AB\rangle$. Let us note that these amplitudes are a function of momenta, as well as the coupling
 109 constant.

110 To quantify the entanglement of these states we use the concurrence as the figure of merit.
 111 It is well-known that in two-level states, as is the case here, all ways of measuring entanglement
 112 reduce to a single combination. Given a two particle pure state

$$|\psi\rangle = \alpha|RR\rangle + \beta|RL\rangle + \gamma|LR\rangle + \delta|LL\rangle, \quad (2)$$

113 with $\alpha, \beta, \gamma, \delta \in \mathbb{C}$ and $|\alpha|^2 + |\beta|^2 + |\gamma|^2 + |\delta|^2 = 1$, the concurrence is defined as

$$\Delta = 2|\alpha\delta - \beta\gamma|, \quad (3)$$

114 where $0 \leq \Delta \leq 1$. The states with $\Delta = 0$ correspond to product states and the ones with
 115 $\Delta = 1$ to maximal entangled states. Thereby, we will start with initial states where the con-
 116 currence equals 0 and explore if there are any final states where this value is increased to 1.
 117 All the coefficients and, thus, the concurrence are a function of the coupling constant and the
 118 momenta defining the kinematics of the process.

119 3 Tree-level gluon scattering amplitudes

120 The gluon scattering process involves four Feynman diagrams that correspond to s , t , u and
 4-vertex channels, as shown in Fig. 1.

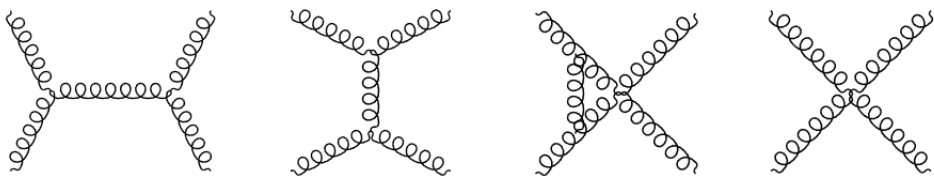


Figure 1: Channels that contribute to the gluon scattering. From left to right, s -channel, t -channel, u -channel and quartic channel.

121
 122 We compute explicitly the amplitudes for the four channels, using the Feynman rules for
 123 these processes. A powerful method to obtain the total polarized amplitudes, that is the spinor
 124 helicity formalism [44], allows to compute scattering amplitudes considering only the exter-
 125 nal particles. It is then possible to get the final amplitudes in a straightforward way, avoiding
 126 long computations. However, we are interested in the relation between the different channels
 127 involved in the scattering process to analyze the detailed mechanisms that generate entangle-
 128 ment. For this reason we do not resort to the spinor helicity formalism.

129 Let us now concentrate on the scattering amplitudes that are not null. The details of the
 130 kinematics, Feynman rules and conventions used are listed in App. A. The complete set of
 131 polarized amplitudes computed for each channel are collected in App. B. Using these values,
 132 the total amplitude is obtained by summing up the amplitudes for each channel

$$\mathcal{M} = \mathcal{M}_s + \mathcal{M}_t + \mathcal{M}_u + \mathcal{M}_4. \quad (4)$$

133 All amplitudes carry a common prefactor involving the coupling constant that will cancel when
 134 computing the concurrence.

135 We shall consider two incoming gluons in a product state of polarizations, $|RR\rangle$, $|RL\rangle$, $|LR\rangle$
 136 or $|LL\rangle$, and momenta p_1 , p_2 and color a , b respectively. After the interaction, we obtain a

137 final state of the form Eq. (1), where the outgoing gluons are characterized by p_3 , p_4 and a' ,
 138 b' , respectively.

139 If the initial state share the same polarization, the interaction does not change the polarization
 140 of the gluons and the final state remains the same product state,

$$\begin{aligned} \mathcal{M}_{RR \rightarrow RR} &= \mathcal{M}_{LL \rightarrow LL} \\ &= 2g^2 \left[f^{abc} f^{a'b'c} \left(\frac{u-t}{s} \right) + f^{aa'c} f^{bb'c} \left(2 + \frac{u-t}{s} \right) \frac{u}{t} + f^{ab'c} f^{ba'c} \left(2 - \frac{u-t}{s} \right) \frac{t}{u} \right], \end{aligned} \quad (5)$$

141 where g is the strong coupling constant and s , t , u the Mandelstam variables defined in Eq.
 142 (22). The values f^{abc} are the structure constants of the $SU(N)$ gauge theory, that are defined
 143 through the commutation relation between its generators $[T_a, T_b] = if^{abc} T_c$. In this scattering
 144 process, there is no generation of entanglement.

145 When the initial product state have opposite polarizations, let it be RL or LR , the interaction
 146 produces a superposition of polarization,

$$\begin{aligned} \mathcal{M}_{RL \rightarrow RL} &= \mathcal{M}_{LR \rightarrow LR} = -2g^2 \left[f^{aa'c} f^{bb'c} \left(\frac{u^2}{ts} \right) + f^{ab'c} f^{ba'c} \left(\frac{u}{s} \right) \right], \\ \mathcal{M}_{RL \rightarrow LR} &= \mathcal{M}_{LR \rightarrow RL} = -2g^2 \left[f^{aa'c} f^{bb'c} \left(\frac{t}{s} \right) + f^{ab'c} f^{ba'c} \left(\frac{t^2}{su} \right) \right]. \end{aligned} \quad (6)$$

147 To simplify the notation, we will use $F_1 \equiv f^{aa'c} f^{bb'c}$ and $F_2 \equiv f^{ab'c} f^{ba'c}$.

148 Using this shorthand notation, we now address the issue to write the amplitudes as re-
 149 stricted to the subspace of two gluons. This can be done by normalizing the state, so that the
 150 colour charge is dropped as well as global factors and signs

$$|\psi\rangle = \frac{1}{\sqrt{N}} \left(\frac{u}{ts} F |RL\rangle + \frac{t}{us} F |LR\rangle \right), \quad (7)$$

151 where we use the shorthand notation $F = F_1 u + F_2 t$, and where the normalization factor is

$$N = \left(\frac{u}{ts} F \right)^2 + \left(\frac{t}{us} F \right)^2 = F^2 \frac{u^4 + t^4}{s^2 t^2 u^2}. \quad (8)$$

152 This normalization makes only sense if the amplitudes are not null due to their color indices.

153 In the case of an initial RL state, the above final amplitudes allow us to cast the effective
 154 final state in the subspace of polarizations in first-order perturbation theory

$$|\psi\rangle_{RL \rightarrow RL+LR} = \frac{1}{\sqrt{t^4 + u^4}} (u^2 |RL\rangle + t^2 |LR\rangle). \quad (9)$$

155 In the case of an initial $|LR\rangle$ state, the result reads

$$|\psi\rangle_{LR \rightarrow RL+LR} = \frac{1}{\sqrt{t^4 + u^4}} (t^2 |RL\rangle + u^2 |LR\rangle). \quad (10)$$

156 A relevant feature in the above result is the cancellation of color degrees of freedom for all
 157 non-zero amplitudes. To be precise, for those color amplitudes which are non-vanishing, the
 158 balance between LR and RL states is not affected by gauge indices. In other words, the final
 159 state generated is the same independently of the color of the gluons involved in the interac-
 160 tion, which implies that the color degrees of freedom are neutral witnesses for any quantum
 161 information quantity computed from the final state wavefunction, including the entanglement
 162 measured with the concurrence or the violation of a Bell inequality. This is in no contradiction

163 with the fact that output colors have different probabilities, as shown in Eq. (6) and dictated
 164 by the color structure functions.

165 The simple form for the scattering of polarizations is the result of cancellations between
 166 the t and u channels vs. the quartic vertex contribution. The s -channel does not generate
 167 entanglement. As a matter of fact, it is never necessary to use the Jacobi identity for the
 168 structure constants. The simple form of the final result emerges for any $SU(N)$ group.

169 4 Generation of entanglement

170 The generation of entanglement in gluon scattering can now be quantified using the concurrence,
 171 defined in Eq. (3). For the final state showed in Eq. (9), we obtain

$$\Delta_{RL \rightarrow RL+LR} = \frac{2t^2u^2}{t^4 + u^4} \quad (11)$$

172 which, in the center of mass frame, corresponds to

$$\Delta_{RL \rightarrow RL+LR} = \frac{2 \tan^4\left(\frac{\theta}{2}\right)}{1 + \tan^8\left(\frac{\theta}{2}\right)}, \quad (12)$$

173 where θ is the COM angle.

174 An identical result is obtained starting from an LR state. Therefore, concurrence for the
 175 polarizations of a process mediated by the strong force only depends on the scattering angle.

176 A first observation about the above result is that concurrence for gluon polarization found
 177 in Eq. (11) takes the exact same form as the one for helicities in identical fermionic scattering
 178 computed in Ref. [2]. There, the contributions from t and u channels are indistinguishable,
 179 bringing the possibility of maximal entanglement for any mass of the fermions. In the case of
 180 gluon dynamics, the variable s is not contributing at all to the amplitude, and the four-vertex
 181 channel cancels some piece of the u and t channels. Thus, although the result is the same for
 182 indistinguishable fermions and for distinguishable colored gluons, the underlying mechanisms
 183 to achieve maximal entanglement are slightly different.

184 To obtain a maximal entangled state, concurrence needs to be $\Delta = 1$. From Eq.(11) it
 185 follows that this happens only when $\theta = \frac{\pi}{2}$, i.e. $t = u$. In this scenario, for every initial
 186 two-gluon product state with opposite polarizations, the final state will be always maximally
 187 entangled, no matter the color charges of the initial state if not identical. Then, the maximal
 188 entangled final states take the form

$$|\psi^+\rangle = \frac{1}{\sqrt{2}} (|RL\rangle + |LR\rangle). \quad (13)$$

189 in both cases. The emergence of the zero component of a triplet is natural due to the fact that
 190 gluons are bosons. In fermionic scattering, the singlet is obtained, showing again the different
 191 nature of both processes.

192 5 Exploring a MaxEnt principle

193 The results obtained for the entanglement in gluon scattering show that the detailed mech-
 194 anism to achieve maximal entanglement is deeply rooted in the interplay between t , u and
 195 quartic-vertex channels. It is natural to explore departures from this fine balance. A more
 196 ambitious point of view can be stated in the form of a principle: The laws of Nature must be

197 able to generate maximal entanglement in scattering processes of incoming particles which
 198 are not entangled. This is tantamount to say that Nature must be exposed to Bell inequalities,
 199 that should be violated. This is to say that Nature should not be describable by a classical
 200 theory. Following Ref. [2], we refer to this idea as a MaxEnt Principle, that may constrain the
 201 structure of interactions.

202 To investigate this idea, we modify the balance between the 3- and 4-gluon interactions.
 203 This is done applying a weight k to the 4-gluon vertex, that leads to a total amplitude

$$\mathcal{M} = \mathcal{M}_s + \mathcal{M}_t + \mathcal{M}_u + k\mathcal{M}_4. \quad (14)$$

204 As we shall discuss shortly, the outcomes for $k \neq 1$ correspond to interactions that are not
 205 gauge invariant. To be precise, we break gauge invariance in the interaction term of the QCD
 206 lagrangian only. Therefore, other Feynman rules such as the gluon propagators, or the gluons
 207 degrees of freedom (they are massless bosons) are not affected by this modification. Although
 208 there are other ways to break gauge invariance, we chose this one as we consider it a minimal
 209 gauge symmetry breaking that allow us to explore the power of imposing MaxEnt in a more
 210 general theory. The values for each amplitude as a function of k are listed in App. C.

211 By repeating the computation in the previous section, we now find that the only value of
 212 k for which the generation of entanglement is independent of the color and for all values of
 213 θ , is the $SU(N)$ gauge invariant case $k = 1$.

214 Let us now concentrate in the case we fix the scattering angle to $\theta = \pi/2$, the concurrence
 215 for any initial polarization becomes independent of the color degree of freedom for any value
 216 of k . In this scenario, the concurrence for initial states of opposite polarizations read

$$\Delta_{RL \rightarrow RL+LR} = \left| \frac{8(k+1)}{5+2k+k^2} \right|. \quad (15)$$

217 The computation shows that only the value $k = 1$ leads to a final maximal entangled state,
 218 i.e. $\Delta = 1$, which corresponds to the theory respecting gauge symmetry. This solution is an
 219 isolated point as shown in Fig. 2, and also suppresses the $LL \rightarrow LL+RR$ process, since

$$\Delta_{RR \rightarrow LL+RR} = \Delta_{LL \rightarrow LL+RR} = 2 \left| \frac{2(k-1)(k-7)}{93-34k+5k^2} \right|. \quad (16)$$

220 These results show how fine-tuned is the gauge invariant Lagrangian for gluon dynamics in
 221 terms of how much entanglement can be created. There are no flat directions. The gauge
 222 invariant theory appears as an isolated point of maximum entanglement with respect to small
 223 variations of the parameter k .

224 It is possible to analyze other scenarios which are departures of the standard theory. For
 225 an initial $|RL\rangle$ polarization, there is a second solution for $k = -3$. Let's write explicitly the
 226 final state as a function of k for an initial $|RL\rangle$ polarization and at $\theta = \pi/2$:

$$|\psi\rangle = \frac{1}{\sqrt{(k-1)^2 + (k+3)^2}} ((k-1)|\phi^+\rangle + (k+3)|\psi^+\rangle), \quad (17)$$

227 where $|\phi^+\rangle = (|RR\rangle + |LL\rangle)/\sqrt{2}$. The final state oscillates between two maximally entangled
 228 states: one that corresponds to an unphysical scenario (as the theory would not obey Ward
 229 identities that preserve the correct degrees of freedom at higher orders of perturbation theory),
 230 $|\phi^+\rangle$, and the QCD solution from Eq. (13).

231 It is also possible to check whether the initial state RR can generate entanglement in a non
 232 gauge invariant theory. In that case, maximal entanglement would be attained at $k = 11/3$.
 233 The final states would be

$$|\psi\rangle = \frac{1}{2\sqrt{5}} (|RL\rangle + |LR\rangle + 3(|RR\rangle - |LL\rangle)). \quad (18)$$

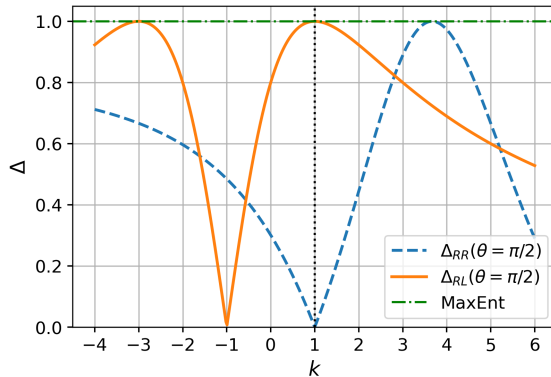


Figure 2: Concurrence as a function of the 4 vertex parameter k and COM angle $\theta = \pi/2$. Maximal entanglement is achieved for the QCD solution $k = 1$ and initial gluon polarization of $|RL\rangle$, but other unphysical solutions are also obtained for $k = -3$ and also for $k = 11/3$ for an initial polarization of $|RR\rangle$. Equivalent results are obtained for initial polarizations $|LR\rangle$ and $|LL\rangle$.

234 A simple rotation of one of the polarizations can show that this state can be transformed into
 235 one of the Bell states.

236 In summary, although a MaxEnt principle in gluon dynamics at tree level is not enough to
 237 completely restrict the gluon interaction to the gauge invariant case, it does single out $k = 1$ as
 238 an isolated point where maximal entanglement is achieved, and gauge symmetry is recovered.

239 6 Conclusions

240 Fundamental interactions generate entangled states by means of indistinguishability of the
 241 relevant degrees of freedom involved.

242 In the case of QED, the superposition of the t and u -channel is at the core of the generation
 243 of entanglement for indistinguishable fermions. In the case particle-antiparticle collisions,
 244 entanglement emerges through the s -channel, where the virtual photon couples identically to
 245 the two options for helicities of the outgoing particles.

246 Gluon dynamics poses a different problem, as in-going, out-going and virtual intermediate
 247 particles are bosons with a color index on top of the polarization. The net effect on the entan-
 248 glement of polarization degrees of freedom requires to add in superposition the contribution
 249 of all s , t , u and quartic-vertex channels. A detailed computation shows that entanglement
 250 among polarizations of the gluons is only generated when the initial product state presents
 251 opposite polarizations. It also shows that maximal entanglement is obtained when outgoing
 252 particles are in the transverse plane.

253 A non-obvious result coming from this computation is that the amount of entanglement
 254 produced in gluon collisions does not depend on the color charge of the gluons. For all com-
 255 binations of initial and final color indices which are allowed, only the scattering angle of the
 256 final state matters, and maximal entangled states arise when $t = u$, that is when the final
 257 gluons trajectories are perpendicular to the initial ones.

258 The generation of maximal entanglement shows that nature is quantum and e.g. QCD
 259 cannot be reproduced by a classical theory based on local determinism. In other words, if
 260 violation of would-be Bell inequalities is mandatory, then gluon dynamics is only describable
 261 by a quantum theory. The production of entanglement in gluon scattering is independent of
 262 the gauge group. However, a small departure of the gauge-tuned relation between the three-

263 and four-gluon vertices would entail a reduction of entanglement. We analyze this possibility
264 by breaking gauge invariance in the interaction term by modifying the balance between the 3-
265 and 4-gluon vertex. Other ways of exploring this gauge symmetry emergence from MaxEnt can
266 be explored, but what we can observe is that those gauge symmetry breaking choices related
267 with the color degrees of freedom will be blind to such modifications. Therefore, even if a
268 possible Principle of MaxEnt does not select a particular gauge group as preferred by Nature,
269 Nature fulfills such a Principle so that universality of entanglement on gauge theories emerges.

270 **7 Acknowledgements**

271 C. N. thanks the Technology Innovation Institute for granting an internship in the Quantum
272 Research Center. A.C.-L. acknowledges funding from Grant RYC2022-037769-I funded by MI-
273 CIU/AEI/10.13039/501100011033 and by "ESF+".

274 **A Conventions**

275 In this section we list all the convention used in this work. We start by stating the kinematics
 276 of the process and then define the Feynman rules used to compute the scattering amplitudes.

277 **A.1 Kinematics**

278 We work in the center of mass (CM) frame, using natural units $c = \hbar = 1$ and the metric
 279 signature $\eta^{\mu\nu} = \text{diag}(+---)$. We consider the process to take place in the xz-plane, with the
 280 momentum of the incoming particles along the z-axis. Then, the momenta are

$$p_1^\mu = (p, 0, 0, p) \\ p_2^\mu = (p, 0, 0, -p), \quad (19)$$

281 for the incoming gluons and

$$p_3^\mu = (p, p \sin \theta, 0, p \cos \theta) \\ p_4^\mu = (p, -p \sin \theta, 0, -p \cos \theta), \quad (20)$$

282 for the outgoing ones, where θ is the scattering angle.

283 The circular polarization vectors for a gluon having a momentum k^μ are defined as

$$\epsilon^\mu(k^\mu, \lambda) = (0, \vec{\epsilon}),$$

284 where

$$\vec{\epsilon} = \frac{-\lambda}{\sqrt{2}} (\cos \theta \cos \phi - i\lambda \sin \phi, \cos \theta \sin \phi + i\lambda \cos \phi, -\sin \theta)$$

285 and $\lambda = \pm 1$, that correspond to R and L, respectively. Then, the polarization vectors for the
 286 gluons having momenta Eq. (19) and Eq. (20) take the form

$$\epsilon^\mu(p_1) = -\frac{\lambda_1}{\sqrt{2}} (0, 1, i\lambda_1, 0) \\ \epsilon^\mu(p_2) = -\frac{\lambda_2}{\sqrt{2}} (0, 1, -i\lambda_2, 0) \\ \epsilon^\mu(p_3) = -\frac{\lambda_3}{\sqrt{2}} (0, \cos \theta, -i\lambda_3, -\sin \theta) \\ \epsilon^\mu(p_4) = -\frac{\lambda_4}{\sqrt{2}} (0, \cos \theta, i\lambda_4, -\sin \theta). \quad (21)$$

287 Each polarization vector is transverse to the corresponding gluon momentum, $\epsilon^\mu(k)k_\mu = 0$,
 288 due to the massless nature of gluons.

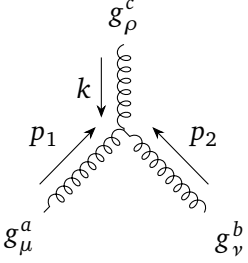
289 Finally, we define the Mandelstam variables as

$$s = (p_1 + p_2)^2 = (p_3 + p_4)^2 \\ t = (p_1 - p_3)^2 = (p_2 - p_4)^2 \\ u = (p_1 - p_4)^2 = (p_2 - p_3)^2, \quad (22)$$

290 where s is the squared center-of-mass energy and t and u are the squared four-momentum
 291 transfer.

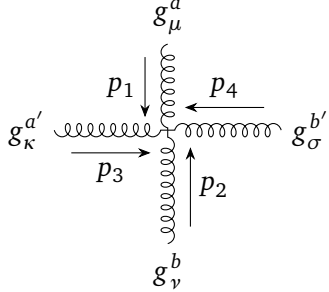
292 **A.2 Feynman rules**

293 Feynman rules are mathematical expressions that represent terms in the Lagrangian of the
 294 theory at work: free external particles and the possible interactions between them. In this
 295 section, we list the Feynman rules of the gluons self-interactions.

296 *Three gluon vertex*

297

$$= g f^{abc} [\eta^{\mu\nu} (p_1 - p_2)^\rho + \eta^{\nu\rho} (p_2 - p_3)^\mu + \eta^{\rho\mu} (p_3 - p_1)^\nu]$$

298 *Four gluon vertex*

299

$$= -ig^2 [f^{abc} f^{a'b'c} (\eta^{\mu\kappa} \eta^{\nu\sigma} - \eta^{\mu\sigma} \eta^{\nu\kappa}) + f^{aa'c} f^{bb'c} (\eta^{\mu\nu} \eta^{\kappa\sigma} - \eta^{\mu\sigma} \eta^{\nu\kappa}) + f^{ab'c} f^{ba'c} (\eta^{\mu\nu} \eta^{\kappa\sigma} - \eta^{\mu\kappa} \eta^{\nu\sigma})]$$

300 **B Polarized amplitudes $gg \rightarrow gg$**

301 Using the Feynman rules in App. A we obtain the amplitudes for each channel. In the following
 302 section we evaluate these amplitudes for the four channels involved in the gluon scattering
 303 process, and obtain the results for all combinations of initial and final polarizations. In all of
 304 them, g is the strong coupling constant, f^{ijk} the structure constants and s, t, u the Mandelstam
 305 variables.

306 **B.1 s -channel**

307 The scattering amplitude of the s -channel takes the form

$$i\mathcal{M}_s = -i \frac{g^2 f^{abc} f^{a'b'c}}{s} \epsilon_\mu(p_1) \epsilon_\nu(p_2) \epsilon_\kappa^*(p_3) \epsilon_\sigma^*(p_4) \\ [\eta^{\mu\nu} (p_1 - p_2)^\rho + 2(\eta^{\nu\rho} p_2^\mu - \eta^{\rho\mu} p_1^\nu)] \\ [\eta^{\kappa\sigma} (p_4 - p_3)^\rho + 2(\eta_\rho^\kappa p_3^\sigma - \eta_\rho^\sigma p_4^\kappa)]. \quad (23)$$

308 The four non-zero amplitudes correspond to the case where both gluons in the initial product
 309 state share the same polarization, and give rise to a final state where, likewise, the polarization
 310 is the same for both gluons. Specifically, these processes correspond to $RR \rightarrow RR$, $RR \rightarrow LL$,
 311 $LL \rightarrow RR$ and $LL \rightarrow LL$, all of which share the same amplitude value,

$$\mathcal{M}_s = g^2 f^{abc} f^{a'b'c} \left(\frac{u-t}{s} \right). \quad (24)$$

312 **B.2 *t*-channel**

313 The scattering amplitude of the *t*-channel takes the form

$$\begin{aligned} i\mathcal{M}_t = & -i \frac{g^2 f^{aa'c} f^{bb'c}}{t} \epsilon_\mu(p_1) \epsilon_\nu(p_2) \epsilon_\kappa^*(p_3) \epsilon_\sigma^*(p_4) \\ & [\eta^{\mu\kappa}(p_1 + p_3)^\rho - 2(\eta^{\kappa\rho} p_3^\mu + \eta^{\rho\mu} p_1^\kappa)] \\ & [\eta^{\nu\sigma}(p_2 + p_4)_\rho - 2(\eta_\rho^\sigma p_4^\nu + \eta_\rho^\nu p_2^\sigma)]. \end{aligned} \quad (25)$$

314 In this case none of them equals zero, but some processes give rise to the same value. We
315 obtain four different values

$$\begin{aligned} \mathcal{M}_{RR \rightarrow RR} &= \mathcal{M}_{LL \rightarrow LL} = -g^2 F_1 \left(2 \frac{4t+u}{s} + \frac{tu}{s^2} \right) \frac{u}{t}, \\ \mathcal{M}_{RL \rightarrow RL} &= \mathcal{M}_{LR \rightarrow LR} = g^2 F_1 \frac{t+2u}{s} \frac{u^2}{ts}, \\ \mathcal{M}_{RR \rightarrow LL} &= \mathcal{M}_{LL \rightarrow RR} = \mathcal{M}_{RL \rightarrow LR} = \mathcal{M}_{LR \rightarrow RL} = g^2 F_1 \frac{t+2u}{s} \frac{t}{s}, \\ \mathcal{M}_{RR \rightarrow RL} &= \mathcal{M}_{RL \rightarrow RR} = -g^2 F_1 \frac{tu}{s^2}, \end{aligned} \quad (26)$$

316 where $F_1 \equiv f^{aa'c} f^{bb'c}$ and we use $s + t + u = 0$.

317 **B.3 *u*-channel**

318 The scattering amplitude of the *u*-channel takes the form

$$\begin{aligned} i\mathcal{M}_u = & -i \frac{g^2 f^{ab'c} f^{ba'c}}{u} \epsilon_\mu(p_1) \epsilon_\nu(p_2) \epsilon_\kappa^*(p_3) \epsilon_\sigma^*(p_4) \\ & [\eta^{\mu\sigma}(p_1 + p_4)^\rho - 2(\eta^{\sigma\rho} p_4^\mu + \eta^{\rho\mu} p_1^\sigma)] \\ & [\eta^{\nu\kappa}(p_2 + p_3)_\rho - 2(\eta_\rho^\kappa p_3^\nu + \eta_\rho^\nu 2p_2^\kappa)]. \end{aligned} \quad (27)$$

319 For this channel we also obtain that none of the amplitudes equals zero and that some processes
320 give rise to the same value. As in the *t*-channel, we obtain four different values

$$\begin{aligned} \mathcal{M}_{RR \rightarrow RR} &= \mathcal{M}_{LL \rightarrow LL} = -g^2 F_2 \left(2 \frac{4u+t}{s} + \frac{tu}{s^2} \right) \frac{t}{u}, \\ \mathcal{M}_{RL \rightarrow LR} &= \mathcal{M}_{LR \rightarrow RL} = g^2 F_2 \frac{2t+u}{s} \frac{t^2}{us}, \\ \mathcal{M}_{RR \rightarrow LL} &= \mathcal{M}_{LL \rightarrow RR} = \mathcal{M}_{RL \rightarrow RL} = \mathcal{M}_{LR \rightarrow LR} = g^2 F_2 \frac{2t+u}{s} \frac{u}{s}, \\ \mathcal{M}_{RR \rightarrow RL} &= \mathcal{M}_{RL \rightarrow RR} = -g^2 F_2 \frac{tu}{s^2}, \end{aligned} \quad (28)$$

321 where $F_2 \equiv f^{ab'c} f^{ba'c}$.

322 **B.4 4-point**

323 Lastly, the scattering amplitude of the 4-point channel takes the form

$$i\mathcal{M}_4 = -ig^2[f^{abc}f^{a'b'c}[(\epsilon_1 \cdot \epsilon_3^*)(\epsilon_2 \cdot \epsilon_4^*) - (\epsilon_1 \cdot \epsilon_4^*)(\epsilon_2 \cdot \epsilon_3^*)] \\ + f^{aa'c}f^{bb'c}[(\epsilon_1 \cdot \epsilon_2)(\epsilon_3^* \cdot \epsilon_4^*) - (\epsilon_1 \cdot \epsilon_4^*)(\epsilon_2 \cdot \epsilon_3^*)] \\ + f^{ab'c}f^{ba'c}[(\epsilon_1 \cdot \epsilon_2)(\epsilon_3^* \cdot \epsilon_4^*) - (\epsilon_1 \cdot \epsilon_3^*)(\epsilon_2 \cdot \epsilon_4^*)]]. \quad (29)$$

324 For this channel we obtain five different non-zero values, that are

$$\begin{aligned} \mathcal{M}_{RR \rightarrow RR} &= \mathcal{M}_{LL \rightarrow LL} = g^2 \left(F_3 \frac{u-t}{s} - F_1 \frac{2t+u}{s} \frac{u}{s} - F_2 \frac{2u+t}{s} \frac{t}{s} \right), \\ \mathcal{M}_{RR \rightarrow LL} &= \mathcal{M}_{LL \rightarrow RR} = -g^2 \left(F_3 \frac{u-t}{s} + F_1 \frac{2u+t}{s} \frac{t}{s} + F_2 \frac{2t+u}{s} \frac{u}{s} \right), \\ \mathcal{M}_{RL \rightarrow RL} &= \mathcal{M}_{LR \rightarrow LR} = g^2 (F_1 + F_2) \left(\frac{u}{s} \right)^2, \\ \mathcal{M}_{RL \rightarrow LR} &= \mathcal{M}_{LR \rightarrow RL} = g^2 (F_1 + F_2) \left(\frac{t}{s} \right)^2, \\ \mathcal{M}_{\substack{RR \\ LL}} \rightarrow \substack{RL \\ LR} &= \mathcal{M}_{\substack{RL \\ LR}} \rightarrow \substack{RR \\ LL} = g^2 (F_1 + F_2) \frac{tu}{s^2}, \end{aligned} \quad (30)$$

325 where $F_3 \equiv f^{abc}f^{a'b'c}$.326 **C Total amplitudes with vertex modification**327 In this section we list the total scattering amplitudes obtained when adding a weight k to the
328 4-gluon vertex, Eq. (14).329 We start with the amplitudes that had non-zero value for $k = 1$. We obtain

$$\begin{aligned} \mathcal{M}_{RR \rightarrow RR} &= \mathcal{M}_{LL \rightarrow LL} = \mathcal{M}_{k=1} + \frac{g^2}{2}(k-1) \left(2F_3 \left(\frac{u-t}{s} \right) - F_1 \frac{2u(2t+u)}{s^2} - F_2 \frac{2t(2u+t)}{s^2} \right), \\ \mathcal{M}_{RL \rightarrow RL} &= \mathcal{M}_{LR \rightarrow LR} = \mathcal{M}_{k=1} + g^2(k-1)(F_1 + F_2) \left(\frac{u}{s} \right)^2, \\ \mathcal{M}_{RL \rightarrow LR} &= \mathcal{M}_{LR \rightarrow RL} = \mathcal{M}_{k=1} + g^2(k-1)(F_1 + F_2) \left(\frac{t}{s} \right)^2, \end{aligned} \quad (31)$$

330 where $\mathcal{M}_{k=1}$ are the amplitudes in Eq. (5) and Eq. (6) and $F_1 \equiv f^{aa'c}f^{bb'c}$, $F_2 \equiv f^{ab'c}f^{ba'c}$
331 and $F_3 \equiv f^{abc}f^{a'b'c}$.

332 The remaining amplitudes are

$$\begin{aligned} \mathcal{M}_{RR \rightarrow LL} &= \mathcal{M}_{LL \rightarrow RR} = -\frac{g^2}{2}(k-1) \left(2F_3 \left(\frac{u-t}{s} \right) + F_1 \frac{2t(2u+t)}{s^2} + F_2 \frac{2u(2t+u)}{s^2} \right), \\ \mathcal{M}_{\substack{RR \\ LL}} \rightarrow \substack{RL \\ LR} &= \mathcal{M}_{\substack{RL \\ LR}} \rightarrow \substack{RR \\ LL} = g^2(k-1)(F_1 + F_2) \frac{tu}{s^2}. \end{aligned} \quad (32)$$

333 **References**334 [1] J. S. Bell, *On the Einstein Podolsky Rosen paradox*, Physics Physique Fizika **1**(3), 195–200
335 (1964), doi:10.1103/physicsphysiquefizika.1.195.

336 [2] A. Cervera-Lierta, J. I. Latorre, J. Rojo and L. Rottoli, *Maximal Entanglement in High*
337 *Energy Physics*, SciPost Phys. **3**, 036 (2017), doi:[10.21468/SciPostPhys.3.5.036](https://doi.org/10.21468/SciPostPhys.3.5.036).

338 [3] A. Cervera-Lierta, *Maximal Entanglement: Applications in Quantum In-*
339 *formation and Particle Physics*, arXiv:1906.12099 [quant-ph] (2019),
340 doi:<https://doi.org/10.48550/arXiv.1906.12099>.

341 [4] R. A. Morales, *Tripartite entanglement and Bell non-locality in loop-induced Higgs boson*
342 *decays*, Eur. Phys. J. C **84**(6), 581 (2024), doi:[10.1140/epjc/s10052-024-12921-4](https://doi.org/10.1140/epjc/s10052-024-12921-4), 2403.
343 [18023](https://doi.org/10.1140/epjc/s10052-024-12921-4).

344 [5] S. Fedida and A. Serafini, *Tree-level entanglement in quantum electrodynamics*, Phys. Rev.
345 D **107**, 116007 (2023), doi:[10.1103/PhysRevD.107.116007](https://doi.org/10.1103/PhysRevD.107.116007).

346 [6] M. Blasone, G. Lambiase and B. Micciola, *Entanglement distribution in Bhabha*
347 *scattering with an entangled spectator particle*, Phys. Rev. D **109**, 096022 (2024),
348 doi:[10.1103/PhysRevD.109.096022](https://doi.org/10.1103/PhysRevD.109.096022).

349 [7] M. Blasone, S. D. Siena, G. Lambiase, C. Matrella and B. Micciola, *Complete comple-*
350 *mentarity relations in tree level QED processes*, arXiv:2402.09195 [quant-ph] (2024),
351 doi:<https://doi.org/10.48550/arXiv.2402.09195>.

352 [8] A. Acín, J. I. Latorre and P. Pascual, *Three-party entanglement from positronium*, Phys.
353 Rev. A **63**, 042107 (2001), doi:[10.1103/PhysRevA.63.042107](https://doi.org/10.1103/PhysRevA.63.042107).

354 [9] S. P. Baranov, *Bell's inequality in charmonium decays*
355 $\eta_c \rightarrow \Lambda \bar{\Lambda}$, $\chi_c \rightarrow \Lambda \bar{\Lambda}$ and $J/\psi \rightarrow \Lambda \bar{\Lambda}$, Journal of Physics G: Nuclear and Parti-
356 cle Physics **35**(7), 075002 (2008), doi:[10.1088/0954-3899/35/7/075002](https://doi.org/10.1088/0954-3899/35/7/075002).

357 [10] S. Chen, Y. Nakaguchi and S. Komamiya, *Testing Bell's inequality using charmonium*
358 *decays*, Progress of Theoretical and Experimental Physics **2013**(6), 63A01 (2013),
359 doi:[10.1093/ptep/ptt032](https://doi.org/10.1093/ptep/ptt032).

360 [11] A. J. Barr, *Testing Bell inequalities in Higgs boson decays*, Physics Letters B **825**, 136866
361 (2022), doi:[10.1016/j.physletb.2021.136866](https://doi.org/10.1016/j.physletb.2021.136866).

362 [12] J. A. Aguilar-Saavedra, *Laboratory-frame tests of quantum entanglement in $H \rightarrow WW$* ,
363 *Physical Review D* **107**(7), 076016 (2023), doi:[10.1103/physrevd.107.076016](https://doi.org/10.1103/physrevd.107.076016).

364 [13] J. A. Aguilar-Saavedra, A. Bernal, J. A. Casas and J. M. Moreno, *Testing entangle-*
365 *ment and Bell inequalities in $H \rightarrow ZZ$* , *Physical Review D* **107**(1), 016012 (2023),
366 doi:[10.1103/physrevd.107.016012](https://doi.org/10.1103/physrevd.107.016012).

367 [14] M. Fabbrichesi, R. Floreanini, E. Gabrielli and L. Marzola, *Bell inequalities and quan-*
368 *tum entanglement in weak gauge boson production at the LHC and future colliders*, The
369 *European Physical Journal C* **83**, 823 (2023), doi:[10.1140/epjc/s10052-023-11935-8](https://doi.org/10.1140/epjc/s10052-023-11935-8).

370 [15] A. Bramon and G. Garbarino, *Novel Bell's Inequalities for Entangled $K^0 \bar{K}^0$ Pairs*, Phys.
371 Rev. Lett. **88**, 040403 (2002), doi:[10.1103/PhysRevLett.88.040403](https://doi.org/10.1103/PhysRevLett.88.040403).

372 [16] Y. Takubo, T. Ichikawa, S. Higashino, Y. Mori, K. Nagano and I. Tsutsui, *Feasibility of Bell*
373 *inequality violation at the ATLAS experiment with flavor entanglement of $B^0 \bar{B}^0$ pairs from*
374 *pp collisions*, Phys. Rev. D **104**, 056004 (2021), doi:[10.1103/PhysRevD.104.056004](https://doi.org/10.1103/PhysRevD.104.056004).

375 [17] K. Ehatäht, M. Fabbrichesi, L. Marzola and C. Veelken, *Probing entanglement and testing*
376 *Bell inequality violation with $e^+e^- \rightarrow \tau^+\tau^-$ at Belle II*, Phys. Rev. D **109**, 032005 (2024),
377 doi:[10.1103/PhysRevD.109.032005](https://doi.org/10.1103/PhysRevD.109.032005).

378 [18] C. Severi, C. D. E. Boschi, F. Maltoni and M. Sioli, *Quantum tops at the LHC: from*
379 *entanglement to Bell inequalities*, The European Physical Journal C **82**, 285 (2022),
380 doi:[10.1140/epjc/s10052-022-10245-9](https://doi.org/10.1140/epjc/s10052-022-10245-9).

381 [19] M. Fabbrichesi, R. Floreanini and G. Panizzo, *Testing Bell Inequalities*
382 *at the LHC with Top-Quark Pairs*, Phys. Rev. Lett. **127**, 161801 (2021),
383 doi:[10.1103/PhysRevLett.127.161801](https://doi.org/10.1103/PhysRevLett.127.161801).

384 [20] Y. Afik and J. R. M. d. Nova, *Quantum information with top quarks in QCD*, Quantum **6**,
385 820 (2022), doi:[10.22331/q-2022-09-29-820](https://doi.org/10.22331/q-2022-09-29-820).

386 [21] M. Blasone, F. Dell'Anno, S. De Siena and F. Illuminati, *Entanglement in neutrino*
387 *oscillations*, EPL (Europhysics Letters) **85**(5), 50002 (2009), doi:[10.1209/0295-5075/85/50002](https://doi.org/10.1209/0295-5075/85/50002).

389 [22] S. Banerjee, A. K. Alok, R. Srikanth and B. C. Hiesmayr, *A quantum-information theoretic*
390 *analysis of three-flavor neutrino oscillations: Quantum entanglement, nonlocal and*
391 *nonclassical features of neutrinos*, The European Physical Journal C **75**, 487 (2015),
392 doi:[10.1140/epjc/s10052-015-3717-x](https://doi.org/10.1140/epjc/s10052-015-3717-x).

393 [23] R. A. Morales, *Exploring Bell inequalities and quantum entanglement in vector*
394 *boson scattering*, The European Physical Journal Plus **138**, 1157 (2023),
395 doi:[10.1140/epjp/s13360-023-04784-7](https://doi.org/10.1140/epjp/s13360-023-04784-7).

396 [24] Y. Afik and J. R. M. de Nova, *Entanglement and quantum tomography with*
397 *top quarks at the LHC*, The European Physical Journal Plus **136**, 907 (2021),
398 doi:[10.1140/epjp/s13360-021-01902-1](https://doi.org/10.1140/epjp/s13360-021-01902-1).

399 [25] ATLAS Collaboration, *Observation of quantum entanglement with top quarks at the ATLAS*
400 *detector*, Nature **633**(8030), 542–547 (2024), doi:[10.1038/s41586-024-07824-z](https://doi.org/10.1038/s41586-024-07824-z).

401 [26] CMS Collaboration, *Observation of quantum entanglement in top quark pair production in*
402 *proton-proton collisions at $\sqrt{s} = 13$ TeV*, Reports on Progress in Physics **87**(11), 117801
403 (2024), doi:[10.1088/1361-6633/ad7e4d](https://doi.org/10.1088/1361-6633/ad7e4d).

404 [27] CMS Collaboration, *Measurements of polarization and spin correlation and observation of*
405 *entanglement in top quark pairs using lepton + jets events from proton-proton collisions at*
406 *$\sqrt{s} = 13$ TeV*, Phys. Rev. D **110**, 112016 (2024), doi:[10.1103/PhysRevD.110.112016](https://doi.org/10.1103/PhysRevD.110.112016).

407 [28] M. Fabbrichesi, R. Floreanini, E. Gabrielli and L. Marzola, *Bell inequality is violated in charmonium decays*, Phys. Rev. D **110**, 053008 (2024),
408 doi:[10.1103/PhysRevD.110.053008](https://doi.org/10.1103/PhysRevD.110.053008).

409 [29] M. Fabbrichesi, R. Floreanini, E. Gabrielli and L. Marzola, *Bell inequality is violated in $B^0 \rightarrow J/\psi K^*(892)^0$ decays*, Phys. Rev. D **109**, L031104 (2024),
410 doi:[10.1103/PhysRevD.109.L031104](https://doi.org/10.1103/PhysRevD.109.L031104).

411 [30] E. Gabrielli and L. Marzola, *Entanglement and Bell Inequality Violation in $B \rightarrow \Phi\Phi$ Decays*,
412 Symmetry **16**(8), 1036 (2024), doi:[10.3390/sym16081036](https://doi.org/10.3390/sym16081036).

415 [31] R. Aoude, E. Madge, F. Maltoni and L. Mantani, *Quantum SMEFT tomogra-*
416 *phy: Top quark pair production at the LHC*, Phys. Rev. D **106**, 055007 (2022),
417 doi:[10.1103/PhysRevD.106.055007](https://doi.org/10.1103/PhysRevD.106.055007).

418 [32] C. Severi and E. Vryonidou, *Quantum entanglement and top spin correlations*
419 *in SMEFT at higher orders*, Journal of High Energy Physics **2023**, 148 (2023),
420 doi:[10.1007/jhep01\(2023\)148](https://doi.org/10.1007/jhep01(2023)148).

421 [33] R. Aoude, E. Madge, F. Maltoni and L. Mantani, *Probing new physics through en-*
422 *tanglement in diboson production*, Journal of High Energy Physics **2023**, 17 (2023),
423 doi:[10.1007/jhep12\(2023\)017](https://doi.org/10.1007/jhep12(2023)017).

424 [34] A. Bernal, P. Caban and J. Rembieliński, *Entanglement and Bell inequalities violation in*
425 *$H \rightarrow ZZ$ with anomalous coupling*, The European Physical Journal C **83**, 1050 (2023),
426 doi:[10.1140/epjc/s10052-023-12216-0](https://doi.org/10.1140/epjc/s10052-023-12216-0).

427 [35] M. Fabbrichesi, R. Floreanini, E. Gabrielli and L. Marzola, *Stringent bounds on HWW and*
428 *HZZ anomalous couplings with quantum tomography at the LHC*, Journal of High Energy
429 Physics **2023**, 195 (2023), doi:[10.1007/jhep09\(2023\)195](https://doi.org/10.1007/jhep09(2023)195).

430 [36] F. Maltoni, C. Severi, S. Tentori and E. Vryonidou, *Quantum detection of new physics in*
431 *top-quark pair production at the LHC*, Journal of High Energy Physics **2024**, 99 (2024),
432 doi:[10.1007/jhep03\(2024\)099](https://doi.org/10.1007/jhep03(2024)099).

433 [37] F. Maltoni, C. Severi, S. Tentori and E. Vryonidou, *Quantum tops at circular lepton collid-*
434 *ers*, Journal of High Energy Physics **2024**, 1 (2024), doi:[10.1007/jhep09\(2024\)001](https://doi.org/10.1007/jhep09(2024)001).

435 [38] S. R. Beane, D. B. Kaplan, N. Klco and M. J. Savage, *Entanglement Suppression and*
436 *Emergent Symmetries of Strong Interactions*, Phys. Rev. Lett. **122**, 102001 (2019),
437 doi:[10.1103/PhysRevLett.122.102001](https://doi.org/10.1103/PhysRevLett.122.102001).

438 [39] I. Low and T. Mehen, *Symmetry from entanglement suppression*, Phys. Rev. D **104**, 074014
439 (2021), doi:[10.1103/PhysRevD.104.074014](https://doi.org/10.1103/PhysRevD.104.074014).

440 [40] Q. Liu, I. Low and T. Mehen, *Minimal entanglement and emergent symmetries in low-*
441 *energy QCD*, Phys. Rev. C **107**, 025204 (2023), doi:[10.1103/PhysRevC.107.025204](https://doi.org/10.1103/PhysRevC.107.025204).

442 [41] M. Carena, I. Low, C. E. M. Wagner and M.-L. Xiao, *Entanglement Suppression, Enhanced*
443 *Symmetry and a Standard-Model-like Higgs Boson*, arXiv:2307.08112 [hep-ph] (2023),
444 doi:<https://doi.org/10.48550/arXiv.2307.08112>.

445 [42] K. Kowalska and E. M. Sessolo, *Entanglement in flavored scalar scattering*, Journal of
446 High Energy Physics **2024**, 156 (2024), doi:[10.1007/jhep07\(2024\)156](https://doi.org/10.1007/jhep07(2024)156).

447 [43] J. Thaler and S. Trifinopoulos, *Flavor Patterns of Fundamental Parti-*
448 *cles from Quantum Entanglement?*, arXiv:2410.23343 [hep-ph] (2025),
449 doi:<https://doi.org/10.48550/arXiv.2410.23343>.

450 [44] H. Elvang and Y. Huang, *Scattering Amplitudes in Gauge Theory and Gravity*, Cambridge
451 University Press, ISBN 9781107069251 (2015).